Materials Research Express

PAPER • **OPEN ACCESS**

Dehydration process in 1D ammonium lead halide and mixing of organic cations in hybrid perovskites through mechanosynthesis

To cite this article: Laura Prisinzano *et al* 2020 *Mater. Res. Express* **7** 115503

Materials Research Express

PAPER

Dehydration process in 1D ammonium lead halide and mixing of organic cations in hybrid perovskites through mechanosynthesis

Laura Prisinzano[1], **Davide Delmonte**[2], **Kevin Carlo Ravaglia**[1], **Valentina Vit**[1] **and Lara Righi**[1,2]

[1] Department of Chemistry, Life Science and Environmental Sustainability University of Parma, Parco Area delle Scienze, 17/a, 43124 Parma, Italy

[2] IMEM-CNR, Parco Area delle Scienze, 37/A, 43123 Parma, Italy

E-mail: lara.righi@unipr.it

Keywords: Lead-based perovskites, x-ray diffraction, thermal analysis, mechanosynthesis

Supplementary material for this article is available online

OPEN ACCESS

RECEIVED
21 September 2020

REVISED
6 November 2020

ACCEPTED FOR PUBLICATION
11 November 2020

PUBLISHED
25 November 2020

Abstract

Organic-lead halide perovskites have attracted much attention as a promising material for optoelectronic and photovoltaic applications. However, the broad commercial use of such materials is hindered by their chemical instability. The detrimental processes of degradation often involve the occurrence of hydrated compounds. However, the knowledge of some aspects related to the thermal stability of hydrated lead halides compounds is still very limited. In this work, we report the structural study dealing with the formation of NH_4PbI_3 obtained by removing crystallization water from $NH_4PbI_3\ (H_2O)_2$ with thermal treatment. The hydrated compound is prepared by solvent-free grinding applied on a mixture of NH_4I and PbI_2 powders. Upon heating, the structural evolution of the de-hydration process, monitored by powder x-ray diffraction, consists in the rearrangement of the 1D chains of octahedral PbI_6 units throughout rotations around a specific crystallographic axis. Besides, the fabrication of the solid solution $(CH_3NH_3)_{1-x}(NH_4)_xPbI_3$ with $x = 0, 0.05, 0.10, 0.20$ is attempted with different conditions of mechanosynthesis. The experimental results confirmed the limited solubility of the NH_4^+ group in the methylammonium lead iodate perovskite with a maximal substitution limit of 5%.

Introduction

In the last years, mesoscopic organic-inorganic perovskites ABX_3 with X = Cl, Br or I gathered increasing attention owing to their outstanding photovoltaic performance with power conversion efficiency reaching 25.2% [1, 2]. The growing interest in the use of these hybrid perovskites is due to their unique combination of crucial properties for the massive employment in the photovoltaic (PV) technology: wide band gap tunability with an appropriate choice of metals, halogens and organic cations; a high dielectric coefficient; absorption in the visible spectrum [3, 4]. The semiconductor $CH_3NH_3PbI_3$, methylammonium lead iodide ($MAPbI_3$), represents the prototypical benchmark showing a series of positive aspects mainly related to the sustainable fabrication of solar cells [5–7].

Nevertheless, dispositive based on PV perovskites have life-time extremely low, barely achieving few months even if protected by physical barriers [8, 9]. The degradation of halide perovskite materials mainly rely on the presence of organic cations sensitive to ambient conditions, such as the intensity of the radiation to which the device is exposed, temperature and atmosphere (as a variation in the content of atmospheric oxygen) [10–12]. For instance, after exposure to humidity, $MAPbI_3$ turns into MAI and PbI_2 causing the substantial degradation of the device with a complete suppression of the optoelectronic properties. Actually the identification of the products obtained by humidity-induced decomposition of $MAPbI_3$ and the relative degradation pathway is still matter of debate [13]. The exposure to humidity contributes to the formation of hydrate products such as $MAPbI_3(H_2O)$ or $(MA)_4PbI_6(H_2O)_2$ that cause negative effects on the morphology of the thin films and consequent degradation of the PV properties [2, 14, 15]. Solid solutions of formammidium lead iodide ($FAPbI_3$)

and $MAPbI_3$ are indicated as one of the most promising material for the design of the new generation PV devices. In contrast, it has been demonstrated that the $FAPbI_3$ is subjected to the transformation into $NH_4PbI_3(H_2O)_2$ in conventional ambient conditions [16, 17]. The gradual formation of hydrated compounds is also observed in mixed halide perovskites such as $Cs_xFA_{1-x}Pb(Br_yI_{1-y})_3$ wherein the degradation proceeds with intermediate different byproducts depending on the diverse experimental conditions [18]. The ammonium based NH_4^+ compound plays also an important role in the conversion of porous NH_4PbI_3 polycrystalline deposition into $MAPbI_3$ thin film with stunning morphological properties [19]. The starting hydrated compound is converted in $MAPbI_3$ with the exposure to CH_3NH_3 gas at ambient conditions, opening the avenue to the affordable production of thin films showing enhanced mesoscopic properties [19].

As recent literature highlights, the hydrated compounds in the halide lead-based compounds are observed in limited number of compositions but, they play a crucial role in many aspects of the chemistry of such materials [15–19]. In this perspective, we investigated the decomposition of the hydrated compound $NH_4PbI_3(H_2O)_2$ with the progressive structural transformation into NH_4PbI_3 during heat treatment. We documented the structural evolution triggered by the release of crystallization water molecules involving the concerted rotation of the edge-sharing ribbons composed by octahedral PbI_6 units.

Then, we pursuit the fabrication of solid solutions with nominal $(CH_3NH_3)_{1-x}(NH_4)_xPbI_3$ x = 0, 0.05, 0.10, 0.20 composition following different mechanosynthesis procedures. The experimental results confirmed the limited solubility of NH_4^+ in the perovskite lattice with a maximal amount of 5%. Our findings are in agreement with what suggested by the empirical approach related to the application of the tolerance factor for perovskite structures [20].

Experimental methods

The synthesis of $NH_4PbI_3(H_2O)_2$ was carried out by manual grinding. The compound is obtained by adding a 1:1 mix of PbI_2 and NH_4I powders in a mortar. The powders were ground for 6–5 min sessions for a total of 30 min of grinding. The reaction was attempted by adding few drops of different solvents as lubricant; we tried acetone and water in separated synthesis processes. However, it was found that the addition of such solvents avoided the phase formation by promoting the decomposition and return to the starting reagents, disadvantaging the formation of $NH_4PbI_3(H_2O)_2$. It was therefore found that the best way to obtain the compound was a solvent-free route that earns 100% yield of single phase.

The mechanosynthesis sessions was carried out by using two planetary ball milling systems: (a) Pulverisette 7 Classic Line (Fritsch) planetary ball milling machine, (b) Retsch planetary mill 100. Both milling systems was used with agate pots and a variable number of agate balls. Specially by using the Retsch milling system, we checked different conditions in terms of run per minute (RPM) and duration of milling. All the mechanosynthesis procedures was attempted without the use of solvent or surfactants.

The structural analysis was performed by powder x-ray diffraction PXRD with the Thermo X'TRA diffractometer working with a Cu Kα radiation and equipped with a solid state detector Si(Li) suited to suppress the Kβ radiation. The XRD measurements collected at different temperatures was undertaken by using a TTK450 Anton Paar camera in the temperature range from room temperature RT to 90 °C. Rietveld and fitting refinements was carried out by using Jana2006 suite [21].

Thermal analysis on the hydrated compound was carried out with Perkin Elmer DSC 6000 and TGA 8000 instruments. Differential scanning calorimetry is performed in N_2 atmosphere from 20 to 100 °C wherein the thermogravimetric analysis was made from RT to 130 °C.

UV–vis diffuse reflectance spectroscopy was carried out using a UV–vis spectrophotometer (U-3900).

Results and discussion

The hydrated form of NH_4PbI_3 is prepared after few minutes of simple grinding of the PbI_2 and NH_4I salts in stoichiometric ratio. The pale yellow microcrystalline powder obtained by mechanosynthesis is analyzed by powder x-ray diffraction.

The collected diffraction pattern corresponds to the sequence of reflections typical of $NH_4PbI_3(H_2O)_2$ in agreement with the PDF 00-074-0397 phase from ICDD (International Center for Diffraction Data) database confirming the absence of secondary phases or residual reagents.

The orthorhombic structure is isostructural with $KPbI_3(H_2O)_2$ and $RbPbI_3(H_2O)_2$ whose crystal data was firstly reported by D. Bedlivi *et al* [22] and determined by single crystal x-ray diffractometry. The ammonium-based system $NH_4PbI_3(H_2O)_2$ crystallizes in space group *Pnma* [20, 21], and forms thin pale yellow needles very similar to the anhydrous $CsPbI_3$ crystals [23]. Therefore, the Rietveld refinement performed on the XRD pattern confirms for the fabricated hydrated ammonium lead iodide the main structural features resumed in the former

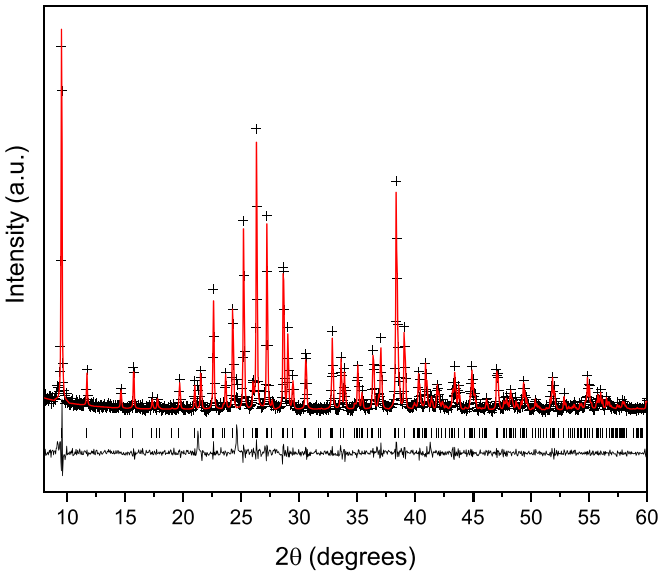

Figure 1. Rietveld plot for the compound $NH_4PbI_3(H_2O)_2$. The ticks indicate the calculated position of the reflections related to the orthorhombic structure. (red line –calculated, black cross- experimental data).

Table 1. Crystal data of $NH_4PbI_3(H_2O)_2$ from Rietveld refinement on x-ray diffraction data collected at RT.

Chemical composition		$NH_4PbI_3(H_2O)_2$		
Symmetry		Orthorhombic		
Space group		P n m a		
a(Å)		10.2589(5)		
b(Å)		4.6115(1)		
c(Å)		22.613(1)		
Z		4		
Rp, Rwp		0.0426, 0.0469		
Atom type	Wck	x	y	z
Pb	4c	0.544(2)	0.25	0.405(3)
I1	4c	0.416(1)	0.25	0.283(2)
I2	4c	0.755(1)	0.25	0.868(3)
I3	4c	0.661(2)	0.25	0.550(2)
NH4	4c	0.136(6)	0.75	0.302(7)
O1	4c	0.042(5)	0.25	0.354(8)
O2	4c	0.063(4)	0.25	0.474(5)

study. Crystal data and agreement factors of the Rietveld analysis, illustrated in figure 1, are summarized in table 1 and selected interatomic distances are listed in table S1. The crystal structure is formed by double chains of edge-sharing PbI_6 octahedra intercalated with NH_4^+ cations. The two symmetrically independent H_2O molecules are longitudinally accommodated along the *c* axis, between the adjacent 1D lead iodide PbI_6 infinite stripes as it is shown in figure 2. Since the starting structural model used for the Rietveld refinement pertains the crystal structure of the counterpart $KPbI_3(H_2O)_2$, [23, 24] the fractional coordinates omits hydrogens for both ammonia group and water molecules (not determined in all the previous structural studies concerning the hydrated lead-based halide compounds). Thus, the analysis of hydrogen-bonds likely occurring in the lattice framework is bypassed. Nevertheless, the O1…O2 distance around 2.72(14) Å is consistent with the occurrence of intermolecular hydrogen bond. Moreover, the N1..O1 length ranging 2.80(9)Å corresponds to a single weak hydrogen bond. The distorted octahedral environment of Pb^{2+} is featured by a long apical Pb–I distance of 3.49 Å (see table S2) exceeding the average of the remaining bond lengths.

To determine the decomposition temperature of the hydrated compound, a complete thermal characterization was carried out. The combined DSC/TGA runs, shown in figure 3, indicate the presence of a sharp transition at 78.4 °C with additional broad peak observed at higher temperatures.

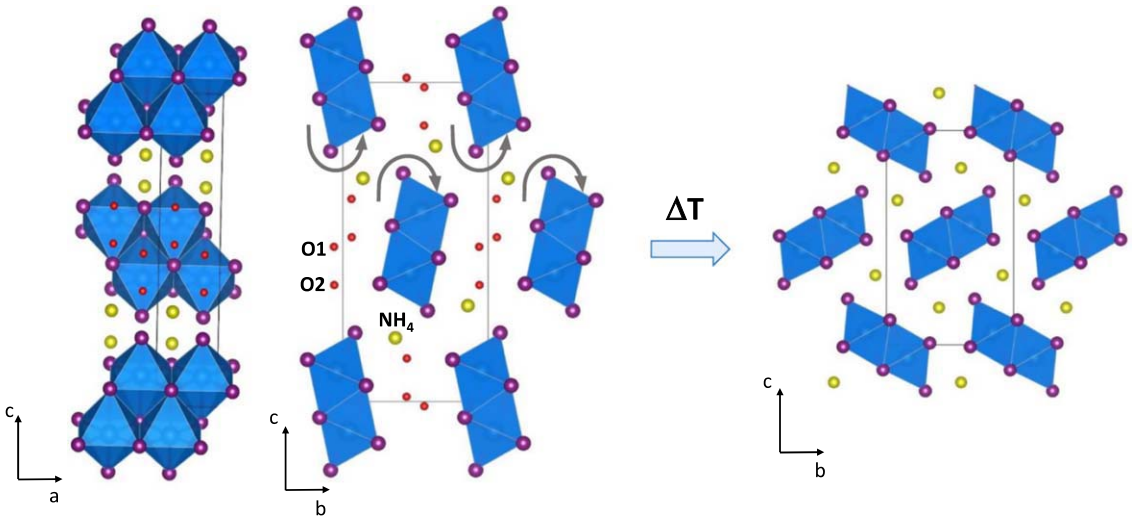

Figure 2. Perspective views of the hydrated (left) and de-hydrated (right) NH_4PbI_3 orthorhombic structures. The double chains of distorted octahedral PbI_6 units are highlighted in blue. The gray arrows defined the clock and anti-clock wise rotation of the ribbons during the dehydration process.

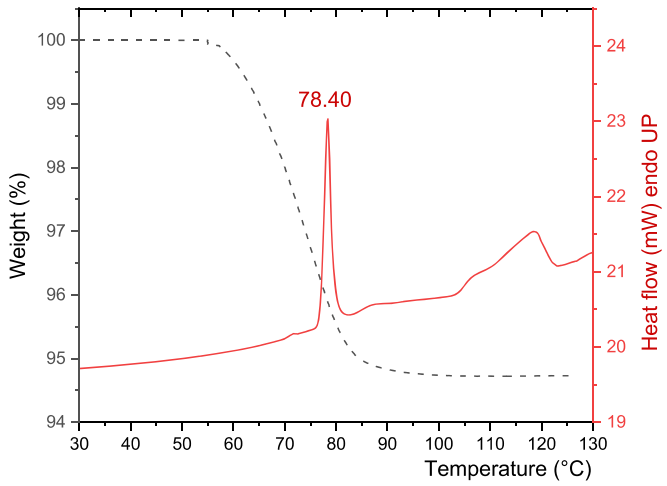

Figure 3. DSC and TGA scan for the $NH_4PbI_3(H_2O)_2$ compound.

The TGA scan reports the marked decrement of weight corresponding to the removal of water molecules from the crystalline phase in the range 68 °C–90 °C. The global weight decrement of 5%, is in agreement with the expected mass of the de-hydrated NH_4PbI_3. Such a temperature transition essentially agrees with the typical thermal conditions found for the dehydration process in other compounds like $RbPbI_3(H_2O)$ and $KPbI_3(H_2O)_2$ [21, 23]. Nevertheless, the relatively low temperature necessary to trigger the transformation is explained by the absence of strong interactions between NH_4^+ and H_2O.

In order to deepen the structural evolution of the de-hydration process we carried out PXRD experiments in the temperature range from RT to 90 °C. To determine the unit cell parameters for both hydrated and de-hydrated NH_4PbI_3 phases the collected diffraction patterns was analyzed by Rietveld method. The dehydrated form is isostructural with NH_4CdCl_3 and the fitting of the unit cell parameters was obtained by adopting the structural model published in [24]. From RT to 60 °C no evident changes are observed in the collected diffraction patterns, in turns by approaching the limit of 68 °C we noticed the rise of a new series of peaks readily attributed to the NH_4PbI_3 orthorhombic phase (see figure S1 available online at stacks.iop.org/MRX/7/115503/mmedia). The figure 4 illustrates the evolution of the unit cell parameters for both phases in the selected 50 °C–90 °C temperature interval. Interestingly, at the first stages of the growth of the stoichiometric NH_4PbI_3 the hydrated phase exhibits a pronounced shortening of the c lattice parameter. This likely indicates a progressive, rather that sudden, release of water molecules predominantly impacting on the longest unit cell constant. Further, the whole structure is progressively distorted as the hydrated phase rapidly decomposes.

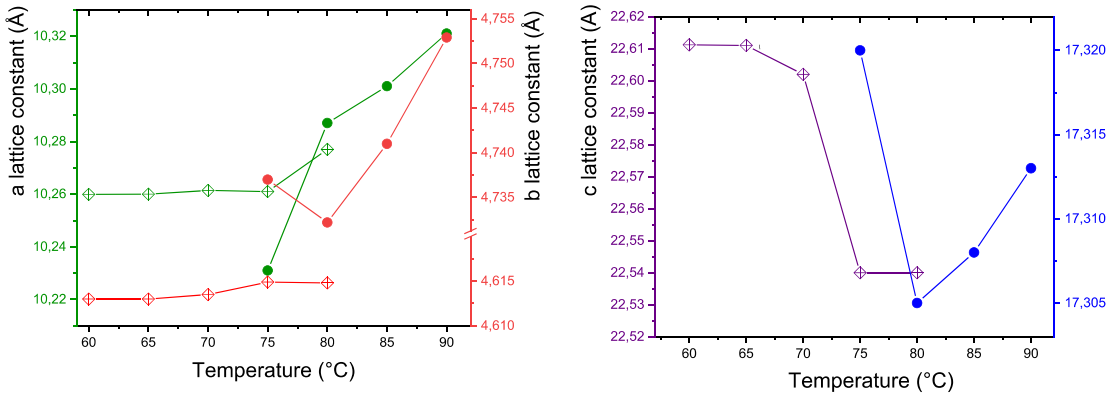

Figure 4. Left: evolution of the *a* and *b* unit cells during the conversion from hydrated to anhydrous NH_4PbI_3 (symbols: open-$NH_4PbI_3(H_2O)_2$, filled-NH_4PbI_3). Right: temperature dependence of *c* parameter.

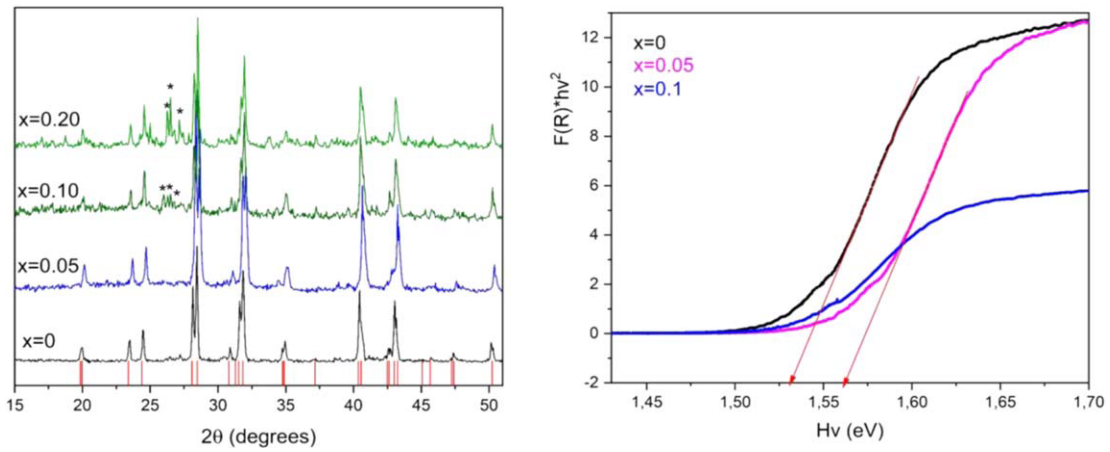

Figure 5. Left: PXRD of the $(MA)_{1-x}(NH_4)_xPbI_3$ system for x = 0, 0.05, 0.1 and 0.2 obtained by 40 min of mechanosynthesis. The stars indicate the reflections corresponding to the hydrated ammonium based compound whereas red ticks define the calculated peaks for the tetragonal phase $MAPbI_3$. Right: Band gap measurement for selected compounds.

The removal of water molecules induces the rotation of the double PbI_6 chains around the a crystallographic axis of about 45°, whilst the NH_4^+ ions shift to occupy interstices originated by the new arrangement of the chains. The double chain located at the origin of the unit cell exhibits an anti-clockwise rotation symmetrical to the clockwise motion involving the second PbI_6 ribbon. Thus three new shorter bonds takes place whereas the longest NH_4^+–I bond (NH_4^+–I1 = 4.00 Å) is broken.

The figure 2 illustrates the main differences of the two structures emphasizing the combined rearrangement of the structural units during the phase transformation.

With the purpose to test the compatibility of NH_4^+ ion in the 3D lead iodate PbI_6 perovskite framework we attempted the fabrication of the solid solution $(MA)_{1-x}(NH_4)_xPbI_3$ with x = 0, 0.05, 0.1 and 0.2. Mechanosynthesis is a solid state method of preparation for nanocrystalline and bulk polycrystalline materials suitable for the achievement of metastable solid solutions that are not attained with classical heat treatments [25, 26]. This unconventional approach is also a powerful tool for activating RT solid state synthesis of inorganic compounds very promising in the field of photovoltaics e.g. Cu–In chalcogenides [25]. For instance, several authors have reported the facile production of optical active lead-based perovskites by mechanochemical procedures [27–29]. The adjustment of some parameters such as milling instrument, energy (rounds per minute RPM), balls-to-powder ratio (BPR) and time requires much attention because they correlate each other [26]. In this work we used two planetary milling systems with a combination of different mechanosynthesis parameters (see table S3). The evolution of the phase formation with time was monitored by collecting small portions of the milled sample at selected moments. In the figure 5, the PXRD patterns for the compounds obtained by the same duration of milling treatment are displayed. The tetragonal $MAPbI_3$ perovskite was obtained as single phase with high-crystallinity degree and their unit cell parameters are listed in the table S4. This systematic study indicated that, irrespectively to the energy of the process, the crystallinity is enhanced as the milling time increases.

Conversely, the mixing of MA^+ and NH_4^+ in the same phase was possible only for minute amount of the NH_4^+ ion.

As it is evidenced in figure 5, as the critical limit of $x = 0.05$ is exceeded, XRD patterns display the presence of the two separated phases namely tetragonal $MAPbI_3$ and hydrated NH_4PbI_3. Indeed, the maximal content of NH_4^+ substituting MA^+ in lead iodate based perovskite is very limited. To evaluate the theoretical stability of the perovskite framework for rational mixing of organic cations, we adopted the tolerance factor approach implemented by G. Kieslich *et al* [30]. The estimation of the tolerance factor indicated as $\alpha = r_x + r_I^- / [\sqrt{2}(r_{Pb}^{2+} + r_I^-)]$ is based on the effective ionic radius for organic cations listed in [30]. The empirical approach based on the geometrical requirements ruling almost close-packed structures indicates that perovskite structure is observed when α parameter corresponds to a value within the 0.91–0.89 range. Considering the $MAPbI_3$ and NH_4PbI_3 endmembers the calculated factor is 0.91 and 0.79 respectively, demonstrating that the ammonium ion NH_4^+ does not possess the size necessary to stabilize the perovskite lattice. If the effective radius is considered with regards to the nominal ratio MA^+/NH_4^+, the maximal amount of NH_4^+ that perovskite can tolerate might be comprised in the 0.1%–8% range. Indeed, for $x = 0.05$, the tolerance factor (0.904) is included in the aforementioned range. In this new compound both *a* and *c* unit cell constants of the tetragonal lattice (see table S3) characterizing $MAPbI_3$ [7, 20, 31] show a significant decrease with a global volume contraction of 1%, clearly indicating the inclusion in the A site of NH_4^+ with respect MA^+.

Further, the successful mechanosynthesis of the $(MA)_{0.95}(NH_4)_{0.05}PbI_3$ compound is also corroborated by band gap (BG) measurements. Figure 5 reports the BG for pure $MAPbI_3$ is 1.52 eV which is in agreement with the previous reported values [32, 33]. Among the series of mixed compounds, we noticed a consistent shift of the band gap for the $x = 0.05$ composition. The widening of the band gap could be related to the structural distortion seemingly involving octahedra tilting. The tuning of the band gap mediated by tilting of octahedral framework and related to the substitution of organic cations was already envisaged by different authors in systematic studies of lead halides based perovskites [34, 35]. As the critical value of x is exceeded, the BG does not show further shift toward higher energy indicating that, irrespective to the nominal composition, the substitution of MA^+ with NH_4^+ is essentially the same for all the mixed compounds.

Furthermore, our study on the replacement of MA^+ with NH_4^+ is in agreement with the results reported by G Wu *et al* on the same system [35]. The authors report the presence of a stable perovskite phase obtained with the incorporation of NH_4^+ in $MAPbI_3$ accompanied by a shift of the observed BG but without indicating the effective degree of substitution achieved [35]. Our findings allow to assess that the limit of substitution of MA^+ with NH_4^+ is closely around 5% and well agrees with the expected constraint indicated by the tolerance factor approach.

Conclusions

The de-hydration process of NH_4PbI_3 was investigated by the combination of thermal and structural characterizations. The removal of water molecules from the orthorhombic structure was investigated giving valuable insights concerning the conversion mechanism from hydrated to anhydrous form. The formation of $MA_{0.95}(NH_4)_{0.05}PbI_3$ perovskite solid solution was undertaken by mechanosynthesis defining a systematic study of the role played by several parameters such as system of milling, rotation speed and duration of treatment. We demonstrated that the NH_4^+ ion is tolerated by perovskite structure with a maximal limit of solubility of around 5%. This result is in line with what predicted by the tolerance factor approach modified for hybrid perovskites [20, 30]. Therefore, in the frame of hybrid organic-inorganic perovskites, our findings point out that this phenomenological approach is a reliable tool for the design of stable solid solutions in hybrid systems.

Acknowledgments

The authors are grateful to Prof. A. Baraldi (University of Parma) for the preliminary measurements of diffuse reflectance spectroscopy band gap. We acknowledge Dr. P. Hernandez (from IMM-CNR Italy) for the additional UV–vis measurements and band gap determination for the whole series of mixed perovskites. The authors thank M. Gemmi (CNI-NEST of Pisa, Italy) for fruitful discussions. E. Gilioli is also thanked for sharing is knowledge on mechanosynthesis processes.

ORCID iDs

Davide Delmonte https://orcid.org/0000-0001-5367-527X
Lara Righi https://orcid.org/0000-0001-9372-5438

References

[1] Lin C 2020 Stabilizing organic–inorganic lead halide perovskite solar cells with efficiency beyond 20% *Front. Chem.* **8** 1–7
[2] Unger E, Paramasivam G and Abate A 2020 Perovskite solar cell performance assessment *J. Phys.: Energy* **2** 044002
[3] Lee S W, Bae S, Kim D and Lee H S 2020 Historical analysis of high-efficiency, large-area solar cells: toward upscaling of perovskite solar cells *Adv. Mater.* **2002202** 1–25
[4] Kojima A, Teshima K, Shirai Y and Miyasaka T 2009 Organometal halide perovskites as visible-light sensitizers for photovoltaic cells *J. Am. Chem. Soc.* **131** 6050–1
[5] Zhang Y *et al* 2020 Ambient fabrication of organic–inorganic hybrid perovskite solar cells *Small Methods* **2000744** 1–40
[6] Motta C, El-Mellouhi F, Kais S, Tabet N, Alharbi F and Sanvito S 2015 Revealing the role of organic cations in hybrid halide perovskite CH_3 NH_3PbI_3 *Nat. Commun.* **6** 7026
[7] Whitfield P S *et al* 2016 Structures, phase transitions and tricritical behavior of the hybrid perovskite methyl ammonium lead iodide *Sci. Rep.* **6** 1–16
[8] Habisreutinger S N, McMeekin D P, Snaith H J and Nicholas R J 2016 Research update: strategies for improving the stability of perovskite solar cells *APL Mater.* **4** 091503
[9] Körbel S, Marques M A L and Botti S 2018 Stable hybrid organic-inorganic halide perovskites for photovoltaics from: *Ab initio* high-throughput calculations *J. Mater. Chem. A* **6** 6463–75
[10] Bisquert J and Juarez-Perez E J 2019 The causes of degradation of perovskite solar cells *J. Phys. Chem. Lett.* **10** 5889–91
[11] Kwak K *et al* 2019 An atomistic mechanism for the degradation of perovskite solar cells by trapped charge *Nanoscale* **11** 11369–78
[12] Wang R, Mujahid M, Duan Y, Wang Z K, Xue J and Yang Y 2019 A review of perovskites solar cell stability *Adv. Funct. Mater.* **29** 1–25
[13] Tolouei nia P, Khassaf H, Shirazi Amin A, Tobin Z M, Alpay S P and Suib S L 2020 Moisture-induced structural degradation in methylammonium lead iodide perovskite thin films *ACS Appl. Energy Mater.* **3** 8240–8
[14] Tran C D T, Liu Y, Thibau E S, Llanos A and Lu Z H 2015 Stability of organometal perovskites with organic overlayers *AIP Adv.* **5** 087185
[15] Gan Z, Yu Z, Meng M, Xia W and Zhang X 2019 Hydration of mixed halide perovskites investigated by Fourier transform infrared spectroscopy *APL Mater.* **7** 031107
[16] Juarez-Perez E J, Ono L K and Qi Y 2019 Thermal degradation of formamidinium based lead halide perovskites into: Sym -triazine and hydrogen cyanide observed by coupled thermogravimetry-mass spectrometry analysis *J. Mater. Chem. A* **7** 16912–9
[17] Van Gompel W T M *et al* 2018 Degradation of the formamidinium cation and the quantification of the formamidinium-methylammonium ratio in lead iodide hybrid perovskites by nuclear magnetic resonance spectroscopy *J. Phys. Chem. C* **122** 4117–24
[18] Marchezi P E *et al* 2020 Degradation mechanisms in mixed-cation and mixed-halide Cs: XFA1- xPb(BryI1- y)3 perovskite films under ambient conditions *J. Mater. Chem. A* **8** 9302–12
[19] Rong Y *et al* 2017 Synergy of ammonium chloride and moisture on perovskite crystallization for efficient printable mesoscopic solar cells *Nat. Commun.* **8** 14555
[20] Oku T 2020 Crystal structures of perovskite halide compounds used for solar cells *Rev. Adv. Mater. Sci.* **59** 264–305
[21] Petříček V, Dušek M and Plášil J 2016 Crystallographic computing system Jana2006: solution and refinement of twinned structures *Zeitschrift fur Krist. - Cryst. Mater.* **231** 583–99
[22] Bedlivy D and Mereiter K 1980 The structures of potassium lead triiodide dihydrate and ammonium lead triiodide dihydrate *Acta Crystallogr. Sect. B Struct. Crystallogr. Cryst. Chem.* **36** 782–5
[23] Sutton R J *et al* 2018 Cubic or orthorhombic? Revealing the crystal structure of metastable black-phase cspbi3 by theory and experiment *ACS Energy Lett.* **3** 1787–94
[24] Haupt H J, Huber F and Preut H 1974 Darstellung und Kristallstruktur von Rubidiumtrijodoplumbat(II) *ZAAC - J. Inorg. Gen. Chem.* **408** 209–13
[25] Fan L Q and Wu J H 2007 NH4PbI3 *Acta Crystallogr. Sect. E Struct. Reports Online* **63** i189
[26] Delmonte D *et al* 2020 An affordable method to produce CuInS2 'mechano-targets' for film deposition *Semicond. Sci. Technol.* **35** 045026
[27] Zyryanov V V, Sadykov V A, Ivanovskaya M I, Criado J M and Neophytides S 2005 Synthesis and sintering of ceramic nanocomposites with high mixed conductivity *Sci. Sinter.* **37** 45–54
[28] Zhu Z Y *et al* 2017 Solvent-free mechanosynthesis of composition-tunable cesium lead halide perovskite quantum dots *J. Phys. Chem. Lett.* **8** 1610–4
[29] El Ajjouri Y, Chirvony V S, Sessolo M, Palazon F and Bolink H J 2018 Incorporation of potassium halides in the mechanosynthesis of inorganic perovskites: feasibility and limitations of ion-replacement and trap passivation *RSC Adv.* **8** 41548–51
[30] Kieslich G, Sun S and Cheetham A K 2014 Solid-state principles applied to organic–inorganic perovskites: new tricks for an old dog *Chem. Sci.* **5** 4712–5
[31] Stoumpos C C, Malliakas C D and Kanatzidis M G 2013 Semiconducting tin and lead iodide perovskites with organic cations: phase transitions, high mobilities, and near-infrared photoluminescent properties *Inorg. Chem.* **52** 9019–38
[32] Dimesso L, Dimamay M, Hamburger M and Jaegermann W 2014 Properties of CH 3 NH 3 PbX 3 (X=I , Br , Cl) Powders as Precursors for Organic / Inorganic Solar Cells *Chem. Mater.* **26** 6762–70
[33] Dimesso L, Wussler M, Mayer T, Mankel E and Jaegermann W 2016 Inorganic alkali lead iodide semiconducting APbI3 (A = Li, Na, K, Cs) and NH4PbI3 films prepared from solution: structure, morphology, and electronic structure *AIMS Mater. Sci.* **3** 737–55
[34] Prasanna R *et al* 2017 Band gap tuning via lattice contraction and octahedral tilting in perovskite materials for photovoltaics *J. Am. Chem. Soc.* **139** 11117–24
[35] Wu C, Guo D, Li P, Wang S, Liu A and Wu F 2020 A study on the effects of mixed organic cations on the structure and properties in lead halide perovskites *Phys. Chem. Chem. Phys.* **22** 3105–11